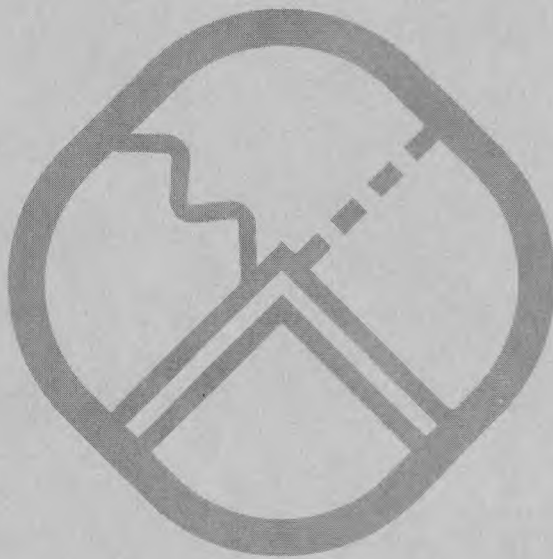


**SELECTIVE DETECTORS FOR
HIGH ENERGY PHOTONS
AND ELECTRONS**

*CLEMENS A. HEUSCH
AND
CHARLES Y. PRESCOTT*

JANUARY 29, 1964



SYNCHROTRON LABORATORY

CALIFORNIA INSTITUTE OF TECHNOLOGY

PASADENA

CALIFORNIA INSTITUTE OF TECHNOLOGY

Synchrotron Laboratory

Pasadena, California

SELECTIVE DETECTORS FOR HIGH-ENERGY

PHOTONS AND ELECTRONS

Clemens A. Heusch and Charles Y. Prescott

January 29, 1964

Supported in part by the U.S. Atomic Energy Commission

Contract No. AT(11-1)-68

CONTENTS

Abstract	p. 2
1. Introduction	p. 3
2. Description of the Counters	p. 4
3. Performance	p. 7
4. Adaptability to Kinematical Requirements	p. 10
5. Determination of Spatial Location of Showers	p. 11
6. Possible Extension of the Method	p. 12
7. Total Energy Measurement	p. 12
8. Conclusions	p. 13
Appendix	
A1. Optimization of Shower Containment	p. 15
A2. Optimization of Shower Buildup	p. 16
A3. Energy Dependence of Shower Distributions	p. 16
A4. Light Collection from Lead Glass Counter	p. 17
A5. Comparison of Light Collection with Different Wrappings	p. 18
A6. Checks on Phototube Linearity	p. 20

ACKNOWLEDGMENTS

We are indebted to R. L. Walker for providing the π and proton beams; to A. V. Tollestrup for his assistance in making suitable electronics available; and to both for interesting and useful discussions. Walter Nilsson skillfully assisted in building the counters. Elliott Bloom was helpful during the test runs.

ABSTRACT

For fast identification of high-energy electrons and photons in heavy backgrounds, a counter was developed consisting of successive layers of lucite and lead. Čerenkov radiation emitted in the lucite slabs is collected onto the photocathode of one 5 inch phototube. The geometry as well as the thickness of inserted lead converters can be adapted to kinematical requirements.

At 1 BeV/c incoming momentum, the rejection ratio of e, γ showers vs. π or μ is better than 100:1; i.e., proper discrimination setting will allow rejection of 99% of all π 's and μ 's, while only 1% of e's and γ 's will be lost. Protons make no pulses at all. The response over the face of the counter is uniform. The properties of the counter are checked in detail against the behavior of lead glass Čerenkov counters, and of lead scintillator sandwiches of comparable geometry. Many applications appear to favor this type of counter over others operating on conventional principles.

1. Introduction

For experimental work around high-energy accelerators, the fast and efficient identification of particles is one of the basic problems. Additional information on energy or momentum of the identified particle is often of equal importance. One phenomenon that sets a class of particles apart is the buildup of electromagnetic showers by high-energy photons and electrons incident on heavy materials, and indeed this property has been frequently used for measurement of photon and electron energies by means of scintillator sandwiches, ionization chambers or lead glass counters, as well as for identification by means of the same instruments and thick-plate spark chambers. All of the mentioned devices have their merits under given circumstances, but for a quick and efficient identification in heavy background, with often changing kinematical requirements, none of these seem to present very satisfactory qualifications (see below). In connection with a given experimental problem of the C.I.T. electron synchrotron, we sought to develop a counter that filled the following requirements:

- A. Recognize high-energy electrons and/or photons in the presence of heavy backgrounds of low-energy e , γ , of π 's, protons, etc.
- B. Give a reasonably accurate information of the energy of the identified γ or electron.
- C. Present a self-defining aperture, eliminating the requirement of extensive shielding.

- D. If possible, make additional aperture or veto counters unnecessary.
- E. Offer easy adaptability to changing kinematical conditions.

In Section 2, we will describe a prototype counter developed to fill these requirements, as well as scintillation and lead glass devices of comparable geometries built to provide a check of the new counter's merits. Section 3 gives the characteristics of the counter's performances in various respects, and a comparison with the other counters. In Sections 4 through 6, we discuss possible adaptations to experimental requirements and combined use of these and other counters. Finally, Section 7 gives the results of a measurement we did to determine the usefulness of these counters for the determination of the energies of incoming photons or electrons. The Appendix describes a number of additional checks and details of possible interest to experimentalists working in the field.

2. Description of the Counters

The geometrical data of the Čerenkov shower counter may be seen from Figure 1. It is composed of six 1/2 inch slabs of

ultraviolet-transmittant lucite, spaced $1/4$ inch apart⁽¹⁾. The light pipe is 2 inches long and feeds the radiation emitted in the six slabs onto the cathode of an RCA 7046 photomultiplier tube (dia. of cathode: 5 inches). The assembled radiator is wrapped in aluminized mylar foil and subsequently covered up with light-tight black tape. This radiator is then joined to the shielded phototube, and the entire counter is solidly mounted in a stand as

(1) The radiator is made in the following way: Cut lucite slabs to slightly oversize [finished sizes: radiators 15 in. (3 in. of which go into the light pipe) x 6 in. x $1/2$ in. or 1 in., spacers (only in light pipe) 3 in. x 6 in. x $1/4$ in.], mill edges roughly, polish only one 6 in. x $1/4$ in. side of spacers. All large faces must be polished (as commercially available). Stack slabs properly, aligning them at the light pipe end, mask polished faces with mylar sheets for protection from glue damage, glue large faces in light pipe section with lucite cement (Plexiglas and Lucite Cement, produced by Fry Plastics International, Los Angeles, California), which has an index of refraction comparable to the lucite's, thus not giving rise to total internal reflection at glued interfaces. Subsequently, let dry for more than one day, then machine, mill edges and turn light pipe part on lathe, sand with fine-grade sandpaper and polish all surfaces to desired quality. The total work takes an experienced laboratory assistant about three days.

illustrated in Figure 2. Into the fully assembled counter lead sheets of adjustable thickness can be inserted; the two slits in the mount of the counters are for insertion of buildup converters in front of the first radiator section.

The sensitive aperture area of this radiator is 10 in. x 6 in., the total thickness of the lucite is 3 in. (three 1-inch sheets for a first prototype counter which was checked quantitatively against a scintillator sandwich and a lead glass counter of comparable geometry; for the final version: six 1/2 in. sheets). Lead sheets of thickness .25 cm, .375 cm and .5 cm were rolled to provide inserts of 1/2, 3/4 and 1 radiation length thickness (in Pb, $1X_0 = .51 \text{ cm}$ or 5.8 gcm^{-2}). Assuming one sheet of $1X_0$ in front of the first radiator section, the total thickness of the counter amounts to $\sim 3X_0$ for the three-layer setup, $6X_0$ for the final one.

In order to check the performance of the counters against counters of more conventional design, we also built a scintillation counter of the same geometry (with lucite light pipes as above), and a lead glass⁽²⁾ counter of comparable thickness. The latter was 7.5 cm ($= 3X_0$) thick, and was used with and without a lucite light pipe (cf. Appendix 4).

(2) Lead glass, type EDF4, from Hayward Scientific Glass Co., Whittier, California; index of refraction: 1.69; one radiation length = 2.5 cm.

3. Performance

To test the counters under well-defined circumstances, we used the monoenergetic electron beam of the 1.5 BeV C.I.T. electron synchrotron (e^- energies variable from $\sim 100 - 1000$ MeV; energy accurate to $\pm 3\%$). For tests involving π 's and protons, the hydrogen target and magnet setup of R.L. Walker was used. Appropriate defining counters determined the beam momentum and the effective aperture of the counter. Coincidences between them opened a fast linear gate, which passed the pulses from the test counter on to a linear integrator-amplifier and into a 256-channel pulse height analyzer.

To intercorrelate all the data obtained, simulated phototube pulses from a pulse generator were fed through the same delay, gate, etc. as the pulses from the counter in order to establish the linearity of the system. Then, all lead was removed from the counters and a check run was taken of passing electrons of $\beta \approx 1$ (cf. Figure 3). Finally, the high voltage on the counter was adjusted so as to make the maximum of this reference distribution fall into one predetermined channel of the pulse height analyzer.

With all lead removed from the counter, high-energy electrons produce the standard distribution shown in Figure 3. The front edge is close to Gaussian, and is determined mainly through the photoelectron statistics at the photocathode of the multiplier tube. The back edge shows a small tail, due mainly to the shower building up in the radiator itself ($\approx .16X_0$), and to

high-energy knock-on electrons. Also shown in Figure 3 are distributions for 500 MeV and 1000 MeV electron showers (see subsequent section). Figure 4, showing the integrated spectra, makes it clear that π 's of comparable momentum behave similarly in the lucite. If, on the other hand, we look at the scintillator sandwich, we find that distributions generated by electrons show a steeper rise in front, indicating the larger amount of light emitted in the scintillation process as compared with the Čerenkov process (also shown in Figure 4). The tail is the same as in the lucite, for electrons; the π 's, however, passing through the scintillation counter (fully stacked with lead) display a tail due to low-energy knock-ons, etc., which the comparable Čerenkov sandwich does not see. For rejection purposes, the shorter tail will obviously be preferable.

Shower Curves

Figure 3 also shows the distributions generated in the lead-stacked counters by 500 and 1000 MeV electrons. Obviously, the amount of light is appreciably larger, but the distributions are wider because of the shower statistics (for optimization of shower distribution, see Appendices 1 and 2). Hence, the shower distributions in the scintillator sandwich look essentially like those from the Čerenkov sandwich.

Rejection Ratios

Figure 5 gives the distributions shown previously in Figure 3, in integrated form. From these we can deduce values for the rejection ratio for 500 and 1000 MeV showers vs. pions. It

is, at 500 MeV, 10:1 (i.e., if one sets the discrimination level to exclude 99% of the pions, 10% of the good showers will be lost). At 1000 MeV, it is better than 100:1 (excluding 99% of the π 's, less than 1% of the 1000 MeV showers will be lost). At higher energies, the ratio will improve over the given number. In the lead-scintillator sandwich (cf. Figure 4), the rejection ratio will be considerably worse at these energies because of the large tail of the π pulse height distribution.

A similar test was made with the lead glass counter. The results are given in Figure 6. Obviously, the poor light collection widens the π distribution, and the long tail makes matters worse. In addition, the high index of refraction of the glass (≈ 1.69) makes protons of comparable momentum give noticeable pulses (absent in lucite radiator).

Light Collection and Uniformity

The above measurements of rejection ratios show that the lead-lucite sandwich array is certainly preferable from that point of consideration. Another argument comes in from a comparison of light collection efficiencies.

If, for the sake of a crude estimate, we consider the quasi-Gaussian front edge of the standard distribution (cf. Figure 3) as determined by the electron statistics on the photocathode, we can find the number of photoelectrons from the parameters defining the Gaussian rise. It turns out to be ≈ 40 . On the other hand, an electron of $\beta \approx 1$ generates in 3 in. of lucite ($n = 1.49$) about 2000 photons in the sensitive frequency range of

the photocathode. Hence, the collection efficiency appears to be as low as 20-30%, if we assume a conversion efficiency of $\approx 10\%$ for the S 11 photocathode.

The number of photons emitted in both the lead glass counters and the scintillator is obviously larger; the better light collection, however, makes for a more uniform distribution over the sensitive aperture in the case of the Pb-lucite counter. If, for the sake of rejection, a discrimination level must be fixed, this is a strong point in favor of the lucite counter. Figure 7 shows a comparison between scans across the faces of the lead glass counter (pulse height maximum varies $\approx 25-30\%$ from top to bottom of counter) and lucite sandwich (pulse height varies $\approx 7\%$)⁽³⁾.

4. Adaptability to Kinematical Requirements

The Čerenkov shower counter offers easy ways to correct for changing kinematical conditions:

(3) An additional check on light collection in the strange geometry of the Pb-lucite sandwich was made by means of running electrons through the light pipe; the ensuing pulse height distribution does not show a marked increase of the "number of photoelectrons" (see above) over the one expected as a consequence of the added lucite thickness. This indicates that the splitting of the radiator into six slabs does not make a large difference on the light collection efficiency.

The effective aperture is defined by the physical dimensions of its sensitive face. To avoid edge effects, the lead inserts and the converter in front of the counter can be shaped so as to allow for minimum shower leakage (cf. Figure 8). The angle of the converter material's grading may be changed according to the distance from γ source (e.g., liquid hydrogen target) to the counter. Pulses stemming from the outside regions of the counter are discriminated against. Pulses due to the passage of particles through the larger lucite thickness of the light pipe may present a problem. In this case, the light pipe has to be shielded from the source. With this exception, aperture shielding should be unnecessary.

For changing energy regions of the electrons or photons that are to be converted, the thickness of the converter material in front of the radiator and of the lead slabs inside can be easily exchanged. (See optimization of thicknesses, Appendices 2 and 3.)

It may be mentioned that building these counters for widely varying geometries does not present a serious problem.

5. Determination of Spatial Location of Showers

If these counters are built to larger sizes, so that their aperture is no longer good enough for the determination of the trajectory of the detected γ or photon, it is possible to use them in conjunction with other apparatus. As indicated in Figure 9, the initial shower buildup material (Pb converter, 1 - $2X_0$ thick)

can be followed by a thin two-gap spark chamber or by a scintillator hodoscope (if one coordinate only is of interest, e.g., the production angle) or two crossed hodoscopes with the required resolutions. The efficiency of this method is simply given by the conversion efficiency of the amount of converter material chosen. Both these systems have been successfully tried out.

In case this is of interest, the shower can likewise be sampled in any gap of the many-layer counter; narrow-gapped spark chambers as well as thin scintillators can be inserted, instead of one slab of lead, between two successive radiator sections.

6. Possible Extension of the Method

For even greater flexibility in adaptation to kinematical requirements, it is possible to build a similar counter in the form of a mirror-walled container filled with an appropriate Čerenkov-radiating liquid. Properly wrapped heavy inserts of all thicknesses can be put in at various locations. This will allow for easier realization of weird shapes (e.g., cylindrical or ellipsoidal) in the vicinity of the target.

7. Total Energy Measurement

In order to test the applicability of our counters to the measurement of the total energy contained in a shower (i.e., the energy of the incoming particle), we had to contain more of the shower than our six-layer counter could hold. Therefore, we assembled two counters in the manner indicated in Figure 10. The

two signals were added after proper matching of the two counters, and subsequently analyzed as above.

Typical pulse height distributions for the output of the front counter (first six radiation lengths) and the back counter are given, for a 1 BeV shower, in Figure 11. Also, the mixed signal is given in the same figure. At 1 BeV, the Gaussian width of the distribution was 12.5%. By building a large counter with more shower containment, and with only one phototube, one could probably improve this resolution somewhat, and avoid the awkward matching necessity for the two tubes.

Even so, the energy resolution will be adequate for many applications, and at 1 BeV is indeed the same as the one given recently by Backenstoss, et.al.⁽⁴⁾ for their large scintillator sandwich operated at CERN. Endeavors to improve on this point are under way.

Figure 12 finally gives the responses of this total-energy system as a function of incident energy. Obviously, at energies above 1000 MeV, shower containment will become poor, and the linearity will not hold any more. Again, improvement on this point should be straightforward to achieve.

8. Conclusions

The Cerenkov shower counter described above appears to

(4) G.Backenstoss, B.D.Hyams, G.Knop and U.Stierlin, Nucl. Inst. and Meth. 21 (1963), 155.

meet all the requirements put forward under 1. In particular, rejection ratios of showering vs. non-showering particles are good and improve with energy. They are naturally superior to those obtainable in other comparable counters like scintillator sandwiches and lead glass γ Cerenkov counters. The light collection is efficient and fairly uniform over large sensitive areas. They are close to self-defining in aperture, with possibly necessary shielding of the light pipe⁽⁵⁾.

The counters are easily adaptable to kinematical and geometrical requirements; they are easy to build in a laboratory and easy to mount and move. In contrast to the conventional sandwich counter with several or many phototubes, no matching of phototubes is necessary, resulting in much greater convenience. The counter's light weight and general ruggedness may make it a good tool for cosmic-ray shower work in balloons and rockets. Last but not least, costs of lucite and of only one phototube make it an inexpensive device. Application of the counter as a total-energy measuring device yields adequate results. Improvements on this point should not be long in coming.

(5) Here is one advantage of a scintillator sandwich of identical geometry: the amount of γ Cerenkov light emitted in the light pipe can be neglected when compared with the scintillator light output.

Appendix

Al. Optimization of Shower Containment

The shower spectra in both the lead glass Čerenkov and the lead lucite sandwich counters have been optimized for the purpose of best rejection ratios as defined above. In order to make the shower spectra as narrow as possible with a large mean pulse height, two parameters can be changed: the amount of lead inserted between the radiator sheets of the PbL counter and the amount of lead used as shower buildup material in front of both the PbL and lead glass counters. Optimum values of both of these parameters will obviously change with the total energy contained in the shower.

The amount of lead (i.e., of active agents for the dissipation of shower energy) within the counter has a fixed value in the lead glass counter; our new device allows for easy change of this parameter. In the energy range considered in this paper ($200 \text{ MeV} \leq E_0 \leq 1000 \text{ MeV}$), we find that a maximum amount of lead within the counter gives the narrowest distributions, i.e., a full radiation length of converter material between each two lucite slabs.

The correlations in the shower structure do not favor the sampling of the shower in as many places as possible, close to the maximum of the average shower⁽⁶⁾, but make maximum shower containment the best way to improve energy resolution.

(6) Average pulse heights will be highest here, but distributions are wide.

A2. Optimization of Shower Buildup

For best values of the rejection ratio, a minimum overlap of the tail of non-showering particles' distribution and the front edge of the shower distribution is desirable (cf. Figure 3). The fluctuations in the structures of individual showers are very large within the first radiation lengths, so that for a steep rise of pulse height distributions of showers in the counters we will have to start sampling the showers at some penetration depth not too close to the front. Series of measurements have been conducted at various energies, adding $1/2$ radiation length of lead in front of the counters at a time. It turns out that a suitable compromise, for the energy range concerned, is met by starting to sample the showers at a penetration depth of $3X_0$ with the lead glass counter, of $2X_0$ with the lead-lucite sandwich. This way, steep front edge rises of the pulse height distributions provide for best attainable rejection ratios, as illustrated in Figures 3, 5 and 6.

A3. Energy Dependence of Shower Distributions

The pulse height distributions from our lead-lucite sandwich counter are shown, for incident electron energies of 200, 300, ... , 1000 MeV, in Figure 13. The lead thickness in front of the counter was $2X_0$ (cf. A2.). The relative width obviously increases with decreasing energy. It is interesting to compare these distributions with those shown in Figure 14, taken with the lead glass counter (buildup thickness in front: $3X_0$). Since the lead glass counter provides for the continuous collection of

^vCerenkov light emitted along the path, whereas the lead-lucite counter simply samples at a number (here: 6) of given penetration depths, one would expect a better-defined, narrower distribution from the lead glass. However, the poor light collection efficiency seems to make matters worse for the lead glass, so that the distributions from the sandwich counter are actually more satisfactory. This detail indicates an important reason for the success of our lead-lucite counter.

A4. Light Collection from Lead Glass Counter

Figure 7 shows that the poor light collection characteristics from the lead glass counter constitute one of its chief disadvantages in the applications discussed here. In order to possibly improve on this point, we have made the following tests:

First we joined the lead glass radiator described in Section 2 directly to the sensitive face of the 5 in. phototube. Next, in order to even out possible effects of light scattering within the radiator, we put a 2 in. lucite light pipe between phototube and lead glass brick. Finally, in order to make up for the effects of short wave lengths of ^vCerenkov radiation reaching the photocathode if emitted close enough (which might account for a sharp rise in pulse height for showers generated in the vicinity of the light pipe or photocathode)⁽⁷⁾, we inserted a light

(7) cf. the confrontation of ^vCerenkov emission spectrum, lead glass transmission and phototube response sensitivity as given by H. Ruderman, R. Gomez, and A.V. Tollestrup, CTSL-31, 1962.

filter⁽⁸⁾ between radiator and light pipe, thus cutting off all wavelengths below about 4000 Å (i.e., that part of the Čerenkov emission spectrum which will be absorbed by passing through any appreciable thickness of lead glass).

The results of these measurements were not encouraging; the presence or absence of the light pipe seemed not to make any noticeable difference. Insertion of the filter improved matters only very slightly. The scan displayed in Figure 7 was taken with a filter.

A5. Comparison of Light Collection with Different Wrappings

Since the amount of light emitted in the lucite radiator is fairly small, a good efficiency of light collection is of importance. We ran a number of tests on different wrappings of the polished radiators in order to optimize reflection conditions. Furthermore, we checked the lucite vs. polystyrene and scintillator plastic to find out comparative transmission data. All geometries were identical, designed to exaggerate the light collection conditions in the sandwich counters: The radiators were 1 in. x 1/2 in. in cross-section, 12 in. long. They were joined directly to the sensitive face of a phototube (RCA 7850), pulse height distributions were taken with a 256-channel analyzer, for three locations of particle passage each: one in the center of the radiator, one at the far end, and one as close to the

(8) Kodak Wratten Gelatine Filters 2C, produced by Eastman Kodak Co.

phototube as the magnetic shielding would permit (≈ 1.5 in. from photocathode). The results are briefly summarized in Table I. It goes without saying that the total amount of light generated in the scintillator is much larger than that generated in the Čerenkov radiators.

The test runs described in Table I were all done in the monoenergetic electron beam, with 500 MeV electrons. They clearly indicate that total internal reflection is the best light collection agent (in the geometry of our counters, most photons will have to undergo many reflections before reaching the photocathode). Destroying total reflection through application of a layer of white paint for overall diffuse reflection makes the radiator act like a photon sink; very careful silvering of the polished surfaces has much the same overall effect, though to a lesser degree. Total internal reflection alone gives fair results (cf. run with black paper wrapping), but both uniformity and average pulse height are considerably enhanced by a highly reflective layer of aluminized mylar foil around the radiator. Further, the results favor UV transmitting lucite (UVT), which was used throughout in our experiment, over the UV absorbing variety (UVA). The polystyrene was added because of its higher index of refraction (1.6 vs. 1.49 for lucite), and ensuing higher photon output. Poor light collection, however, rules it out as a suitable Čerenkov radiator. The collection uniformity for the scintillator is equally inferior. For all the shower data taken, UVT radiator material was used with a wrapping of aluminized mylar (cf. Section 2).

A6. Checks on Phototube Linearity

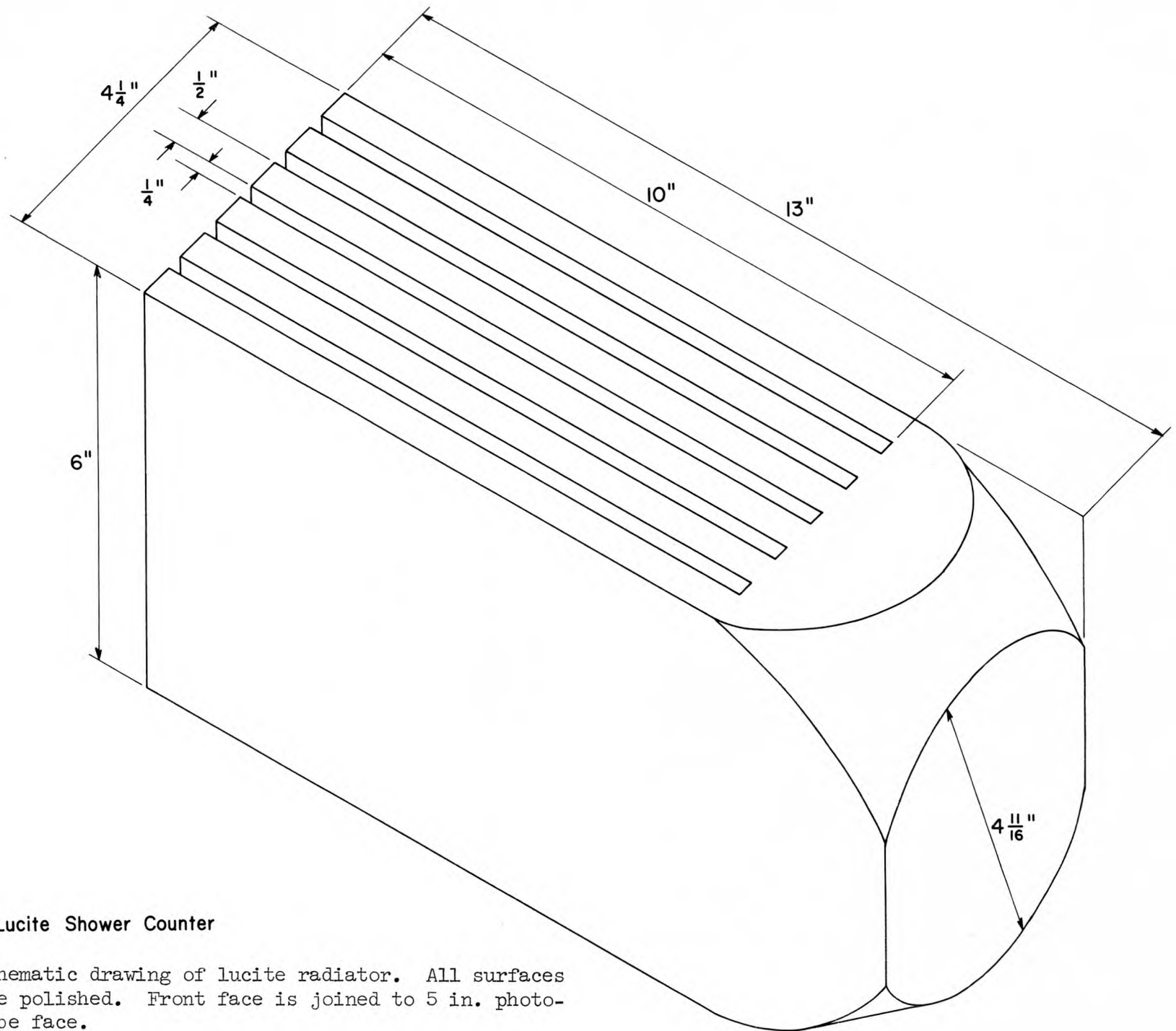
In order to establish the results reported in Sections 3 and 7, checks had to be made on possible non-linearities in the system. The linearity of the electronic circuitry was constantly checked with a pulse generator, as mentioned in Section 2. An additional possible error could stem from non-linear amplification in the phototubes (e.g., saturation effects). We eliminated this source of error by running the phototubes in a light-pulser setup, where the intensity of light incident on the photocathode could be regulated by a polaroid filter, while at the same time matching the phototube's output pulse height with the maximum pulse heights encountered in the experiment. The intensity of light transmitted by the filter is proportional to $\cos^2\theta$, where θ is the angle of the polaroid setting. Figure 15 demonstrates that the mean values of the pulse height distribution generated by the light-pulser rise linearly with intensity. Another check is provided by measurements we did on the development of electromagnetic showers at given incident energies and given penetration depths⁽¹⁰⁾: The apparent number of shower particles at the maximum of the respective average shower spectra rises monotonically, and almost linearly, with E_0 (cf. Figure 16). We wish to enter this last point as qualitative evidence only, without, in this place, entering into the details of shower physics.

(10) cf. C.A.Heusch and C.Y.Prescott, Bull. Am. Phys. Soc. II 8
(1963), 617; to be submitted to Nuc. Phys.

Radiator Material	Wrapping	Average Pulse Height	Uniformity of Collection Efficiency
UVT Lucite	black paper	fair	poor
	painted white	low	very poor
	silvered surface	fairly low	poor
	aluminized mylar foil	high	good
UVA Lucite	aluminized mylar foil	fair	good
Polystyrene	aluminized mylar foil	fair	good
Scintillator Plastic	aluminized mylar foil	very high	fairly poor

Results of model runs for determination of light transmitting properties of various radiators and wrappings. Geometries for all radiators: 1 in. x 1/2 in. x 12 in. All faces polished. Test particles were 500 MeV electrons run through 1/2 in. thickness. Size of defining counter: 1/2 in. x 1/2 in. Phototube directly joined to one end of radiator. Pulse height distributions were taken, for each case, at end close to tube, in middle, and at far end of radiator.

Table I



Prototype of Lucite Shower Counter

Figure 1 - Schematic drawing of lucite radiator. All surfaces are polished. Front face is joined to 5 in. photo-tube face.

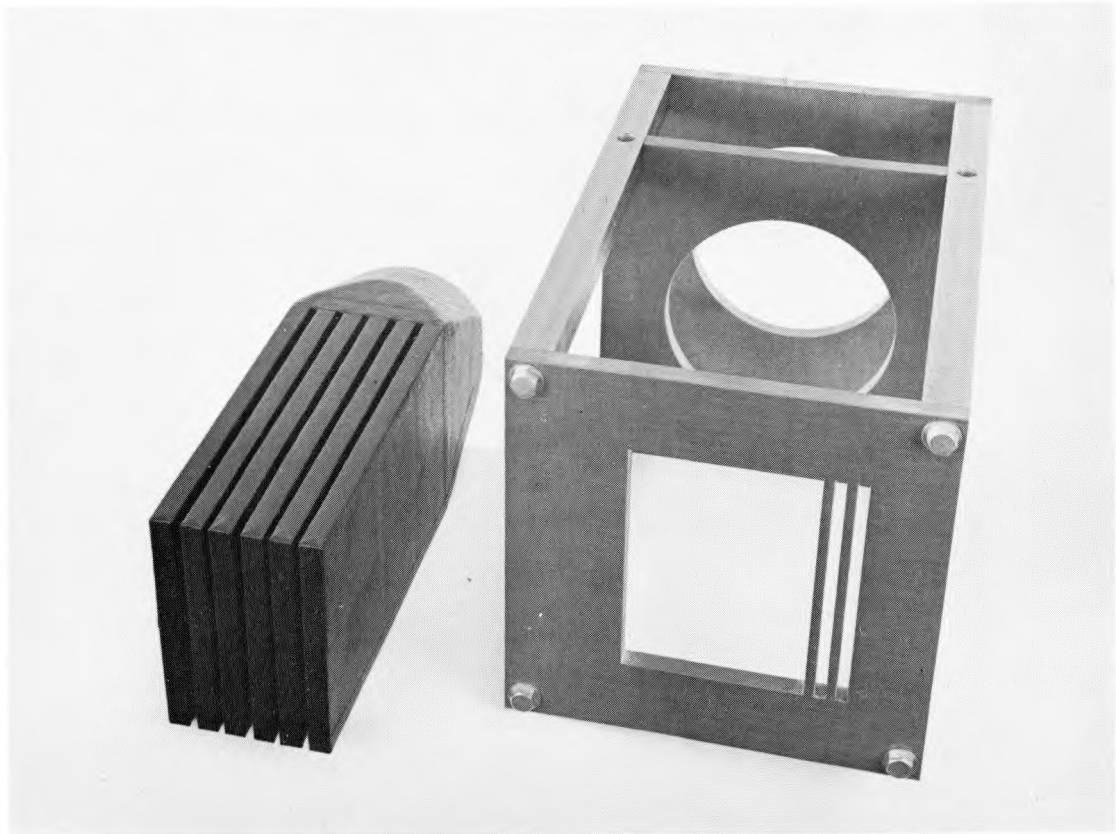
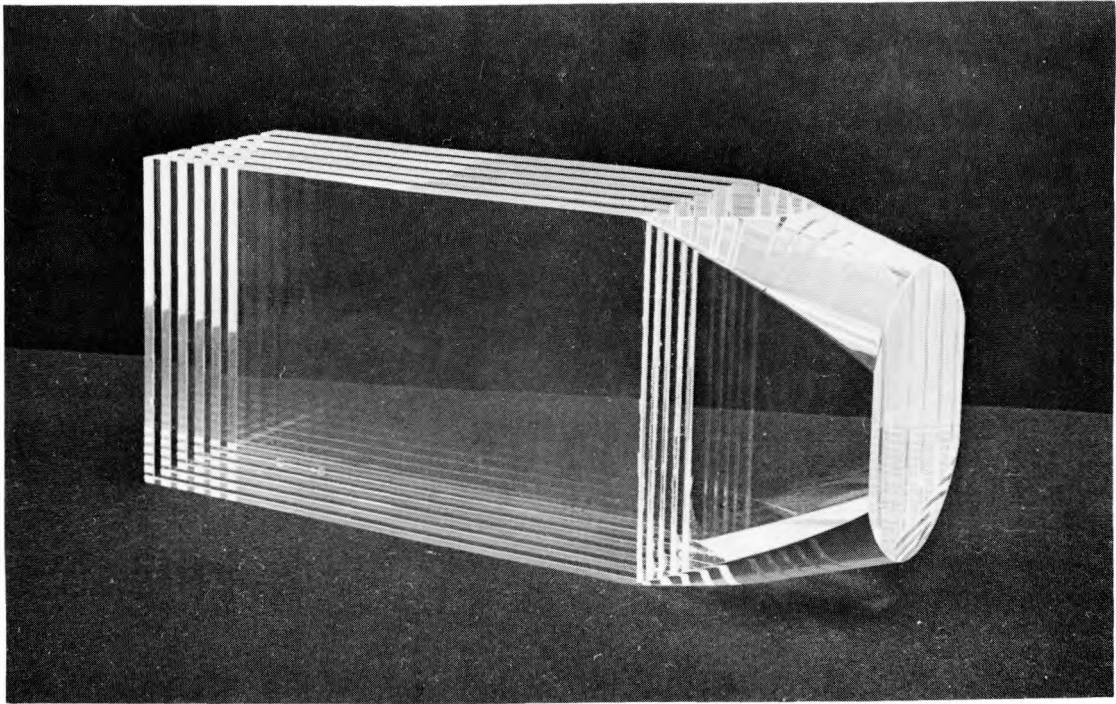


Figure 2 - (a) Lucite radiator, bare (b) left: radiator, wrapped in aluminized mylar foil and light-tight tape; right: mount for assembling radiator (front) and shielded phototube (slide in from back). Slits in front are for insertion of shower buildup material in front of radiator.

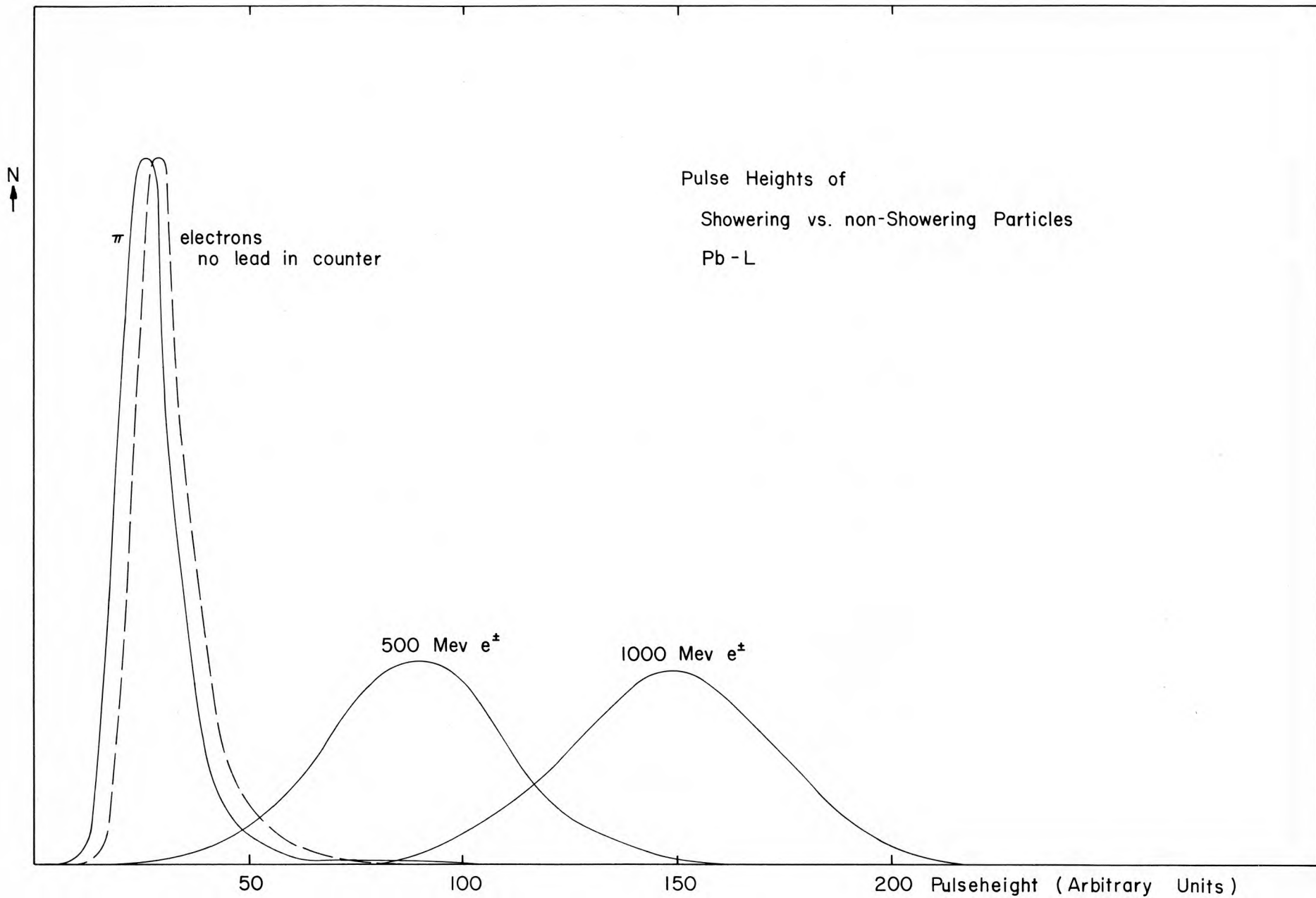


Figure 3 - Pulse height distributions for π 's (800 MeV/c), electrons (500 MeV/c, 1000 MeV/c) from lead-lucite counter; and for electrons from lucite alone, without lead inserts.

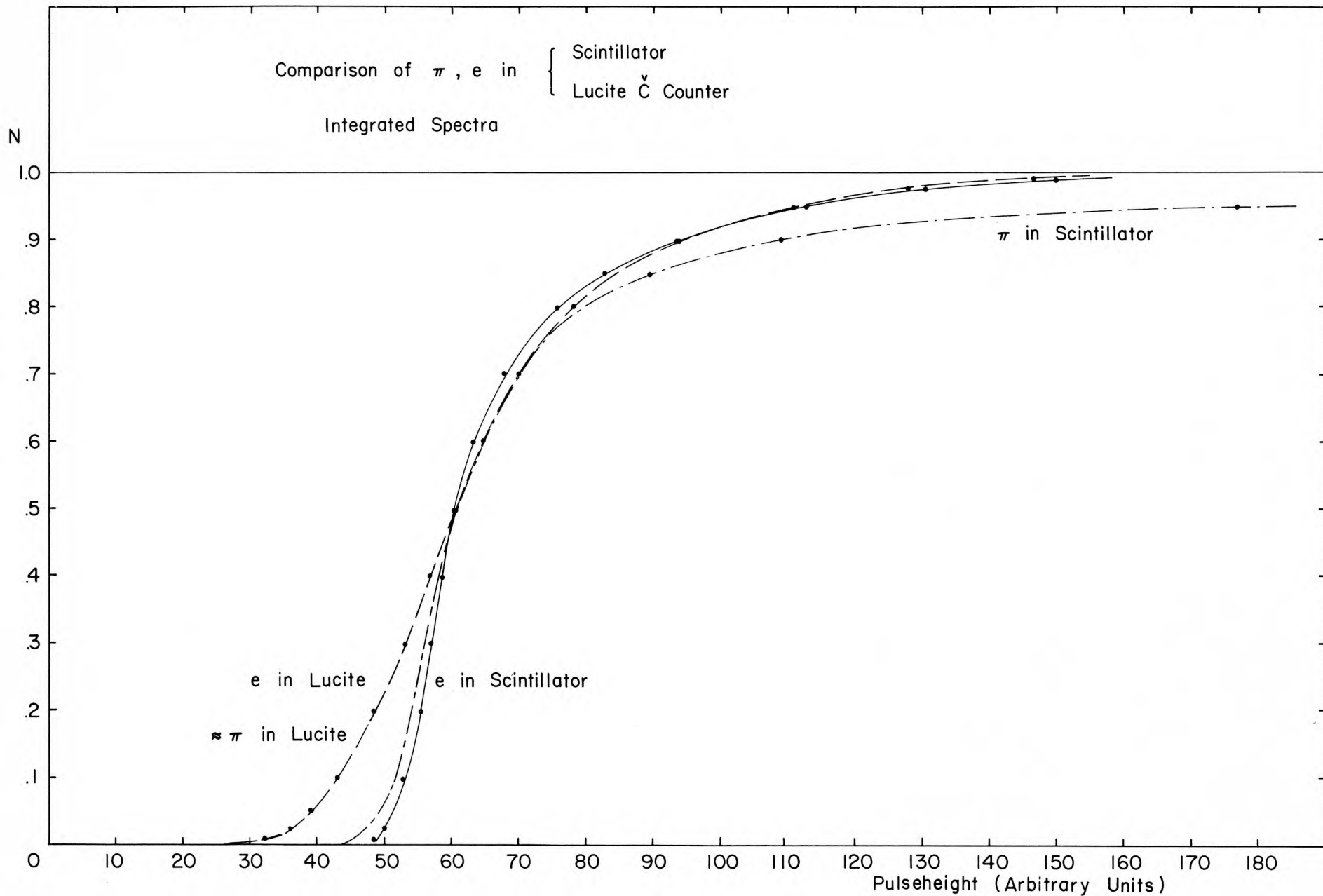


Figure 4 - Integrated pulse height distributions from lucite Cerenkov radiator and scintillator of equal geometries. Electrons and pions show similar behavior in lucite. In scintillator, front rise is similar for π , e, but tails differ widely.

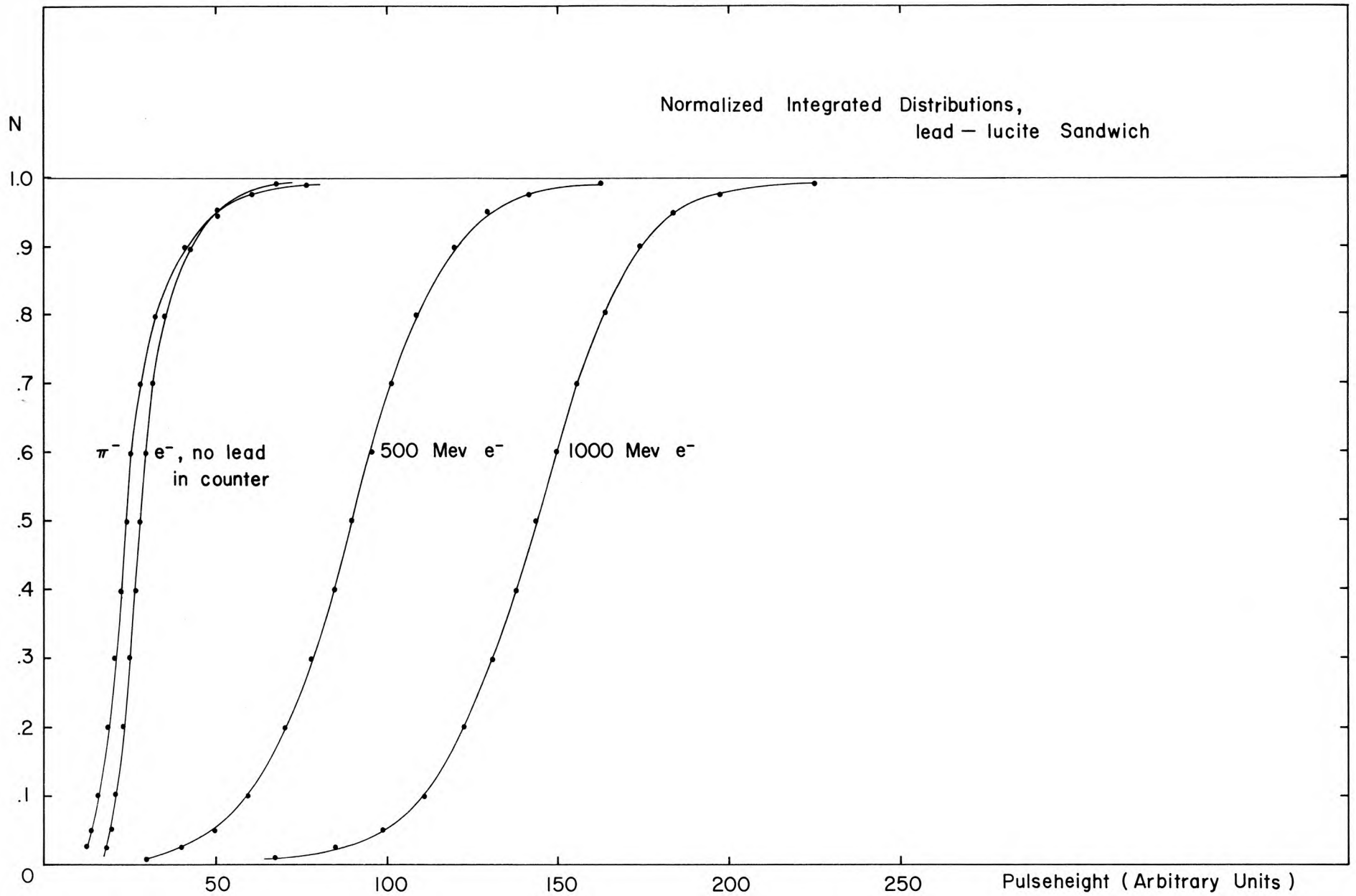


Figure 5 - Integrated pulse height distributions from lead-lucite counters (cf. Figure 3) for given discrimination level, rejection ratios can be read off.

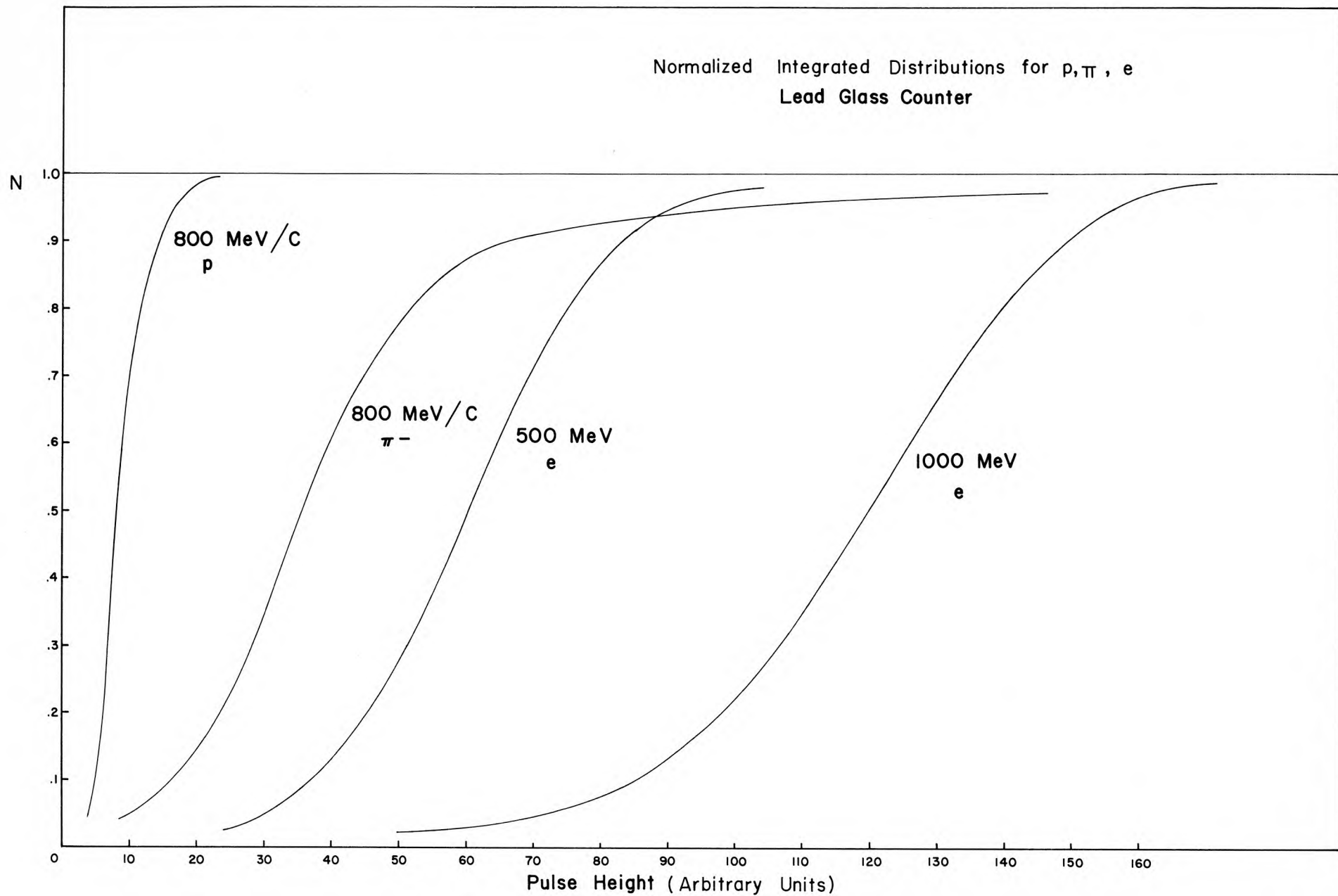


Figure 6 - Integrated pulse height distributions from lead glass counter. Long tail of π distribution makes rejection ratios poor in comparison to PbL counter (Figure 5).

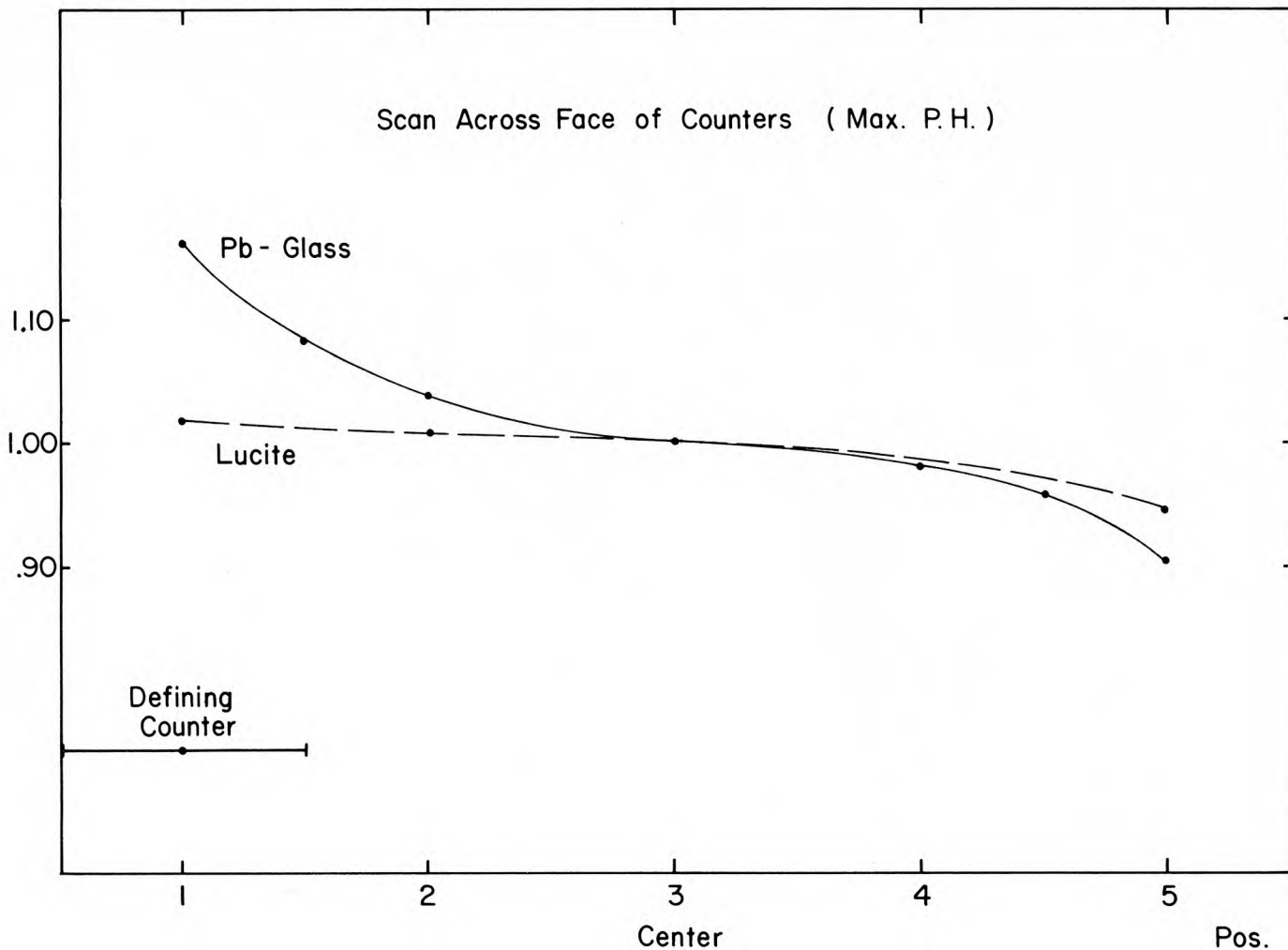
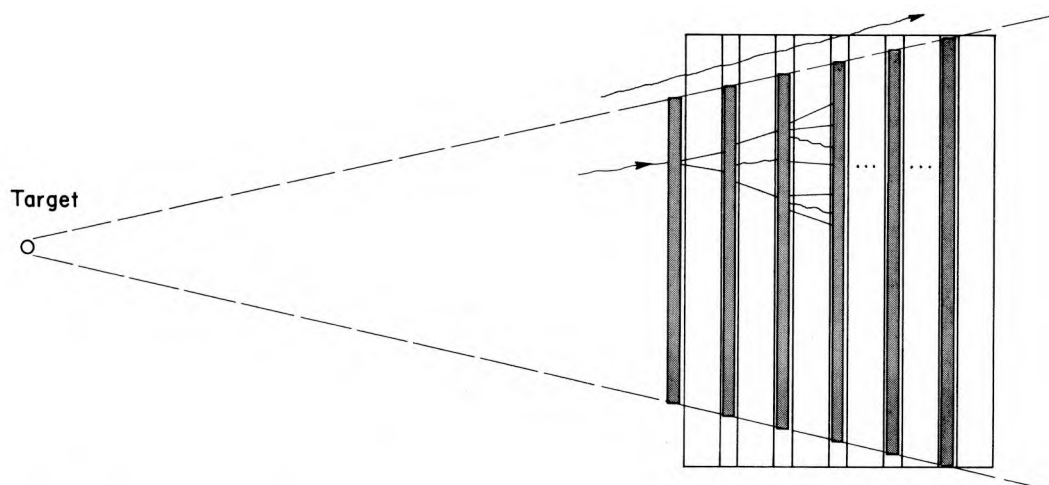


Figure 7 - Comparison of average pulse height generated by electrons of $\beta \approx 1$ passing through different points of PbL and lead glass counters. Uniformity is good for lucite, poor for lead glass. Size of defining counters is shown.



Example of self-defining aperture for Pb-L counter

- ▣ Pb Converter
- Lucite Radiator

Figure 8 - Example of shaping lead inserts for self-definition of counter aperture as seen from point source.

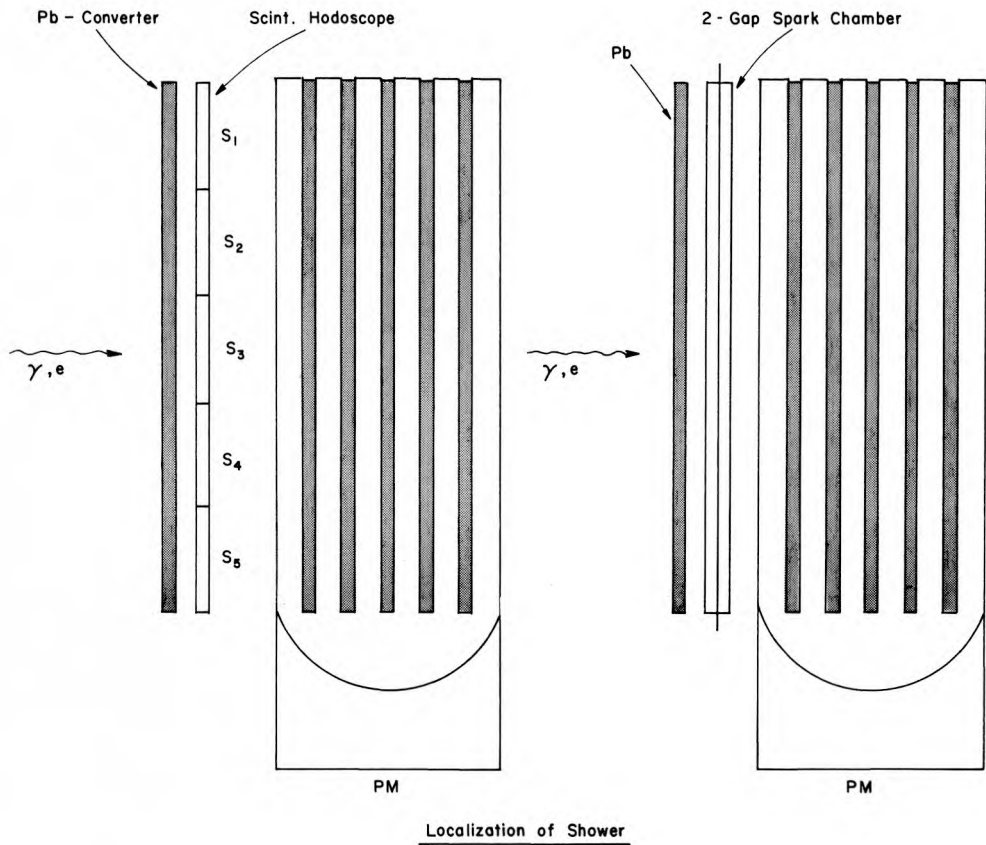


Figure 9 - Schematic view of devices for localization of shower-building particle's trajectory. Left: scintillator hodoscope (could be expanded to two crossed hodoscopes). Right: thin-foil spark chamber with two narrow gaps.

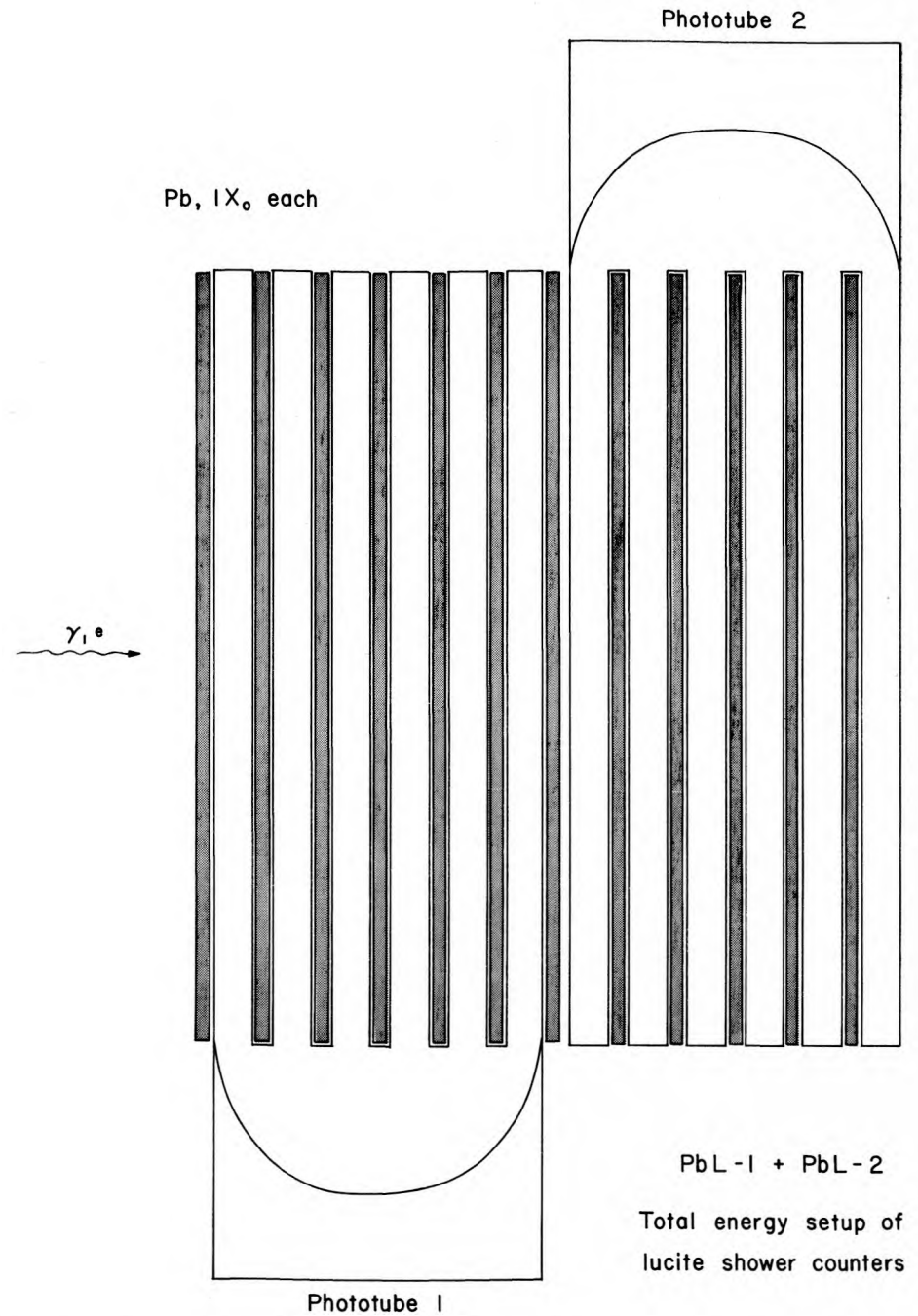


Figure 10 - Schematic view of experimental array for measurement of total shower energy with two consecutive PbL counters. Lead inserts are one radiation length thick each. Total shower containment: $12X_0$.

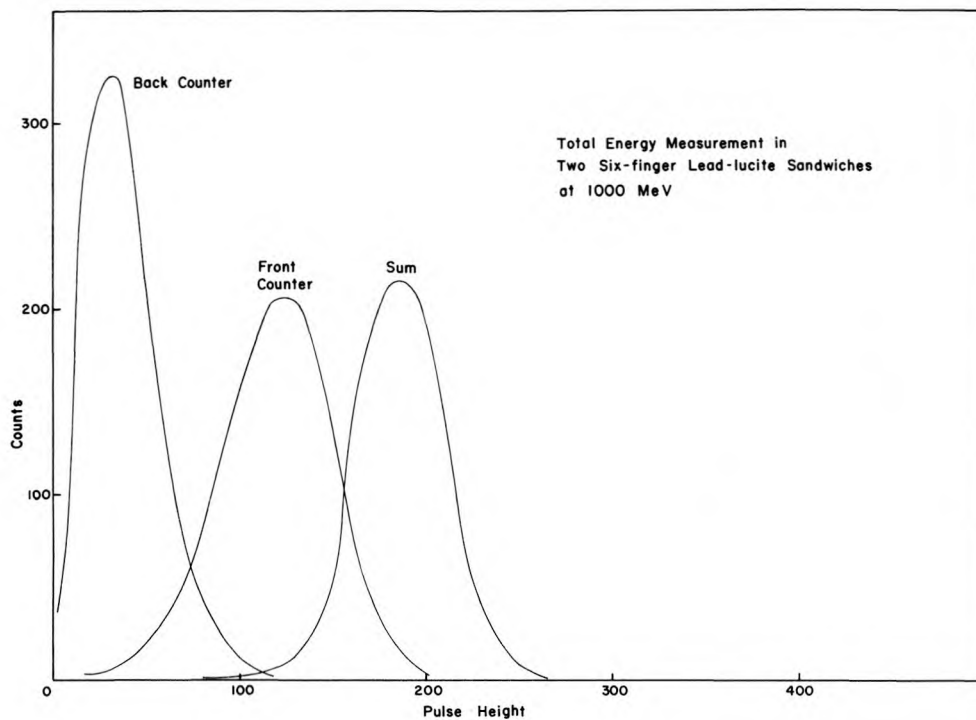


Figure 11 - Pulse height distributions in total absorption measurement (see Figure 10). Front counter exhibits shower spectrum like those displayed in Figure 13. Back counter, looking at tail of average shower, shows ragged distribution. Added signal (gain not exactly = 1) shows marked slimming of shower distribution. Incoming energy: 1 BeV; width of distribution: $\sigma \approx 12.5\%$; full width at half-maximum $\approx 29\%$.

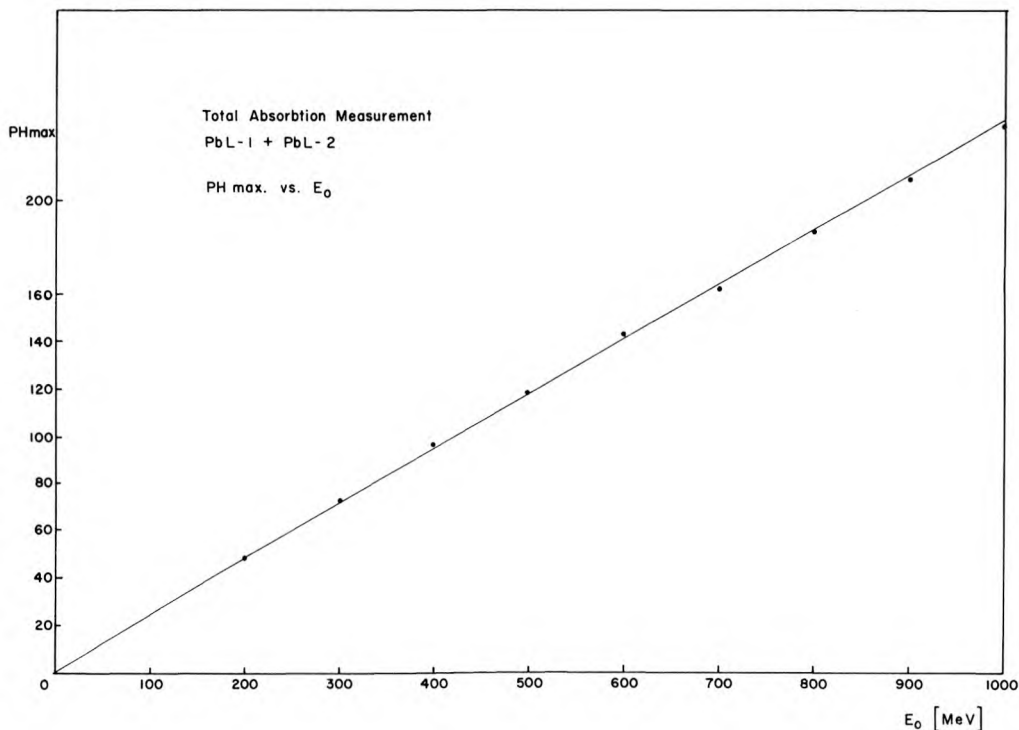


Figure 12 - Dependence of average pulse height of total-energy measurement as a function of incoming energy. Slight non-linearity because of shower leakage is barely noticeable in energy range shown here.

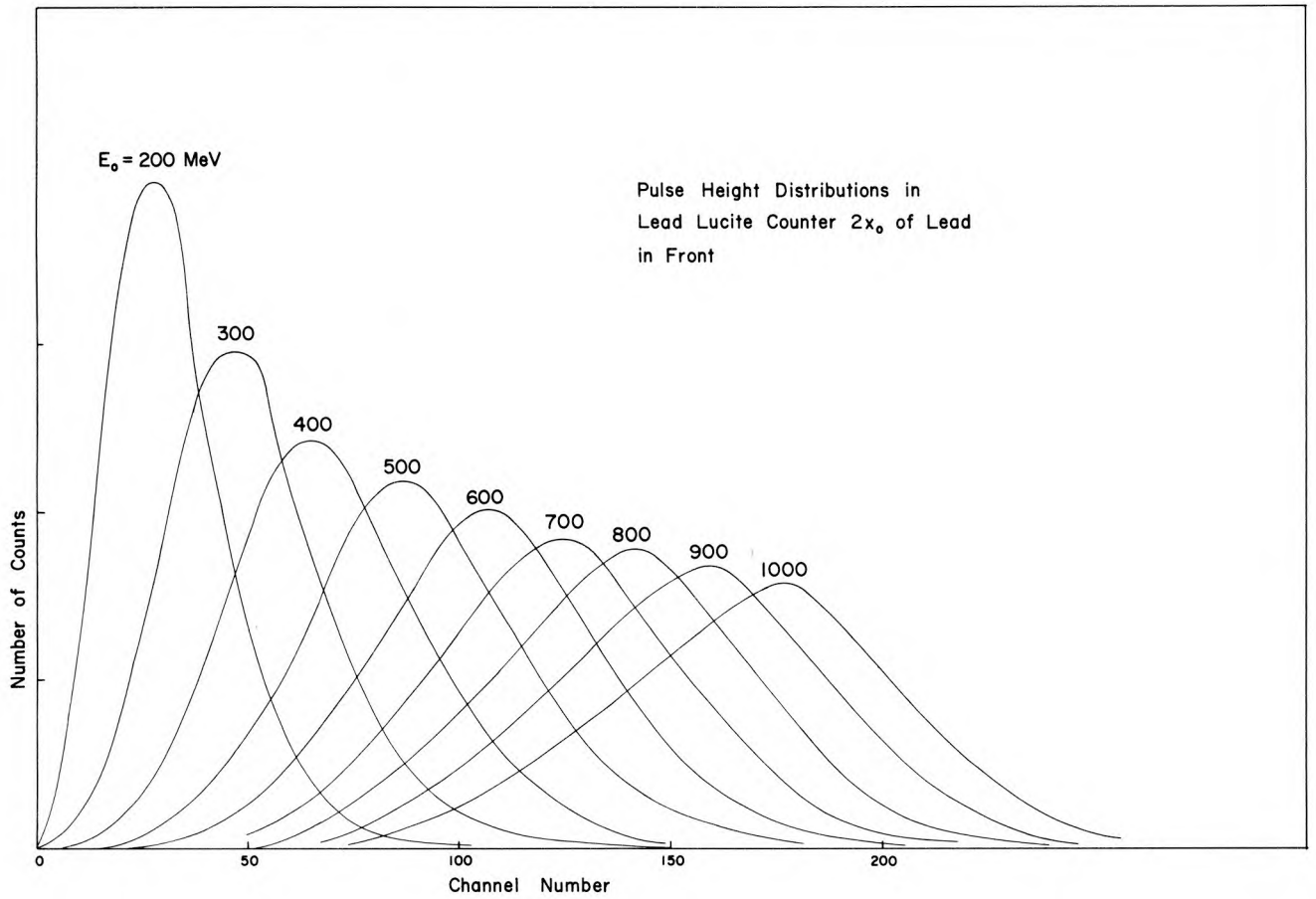


Figure 13 - Shower pulse height distributions from lead-lucite counter: $200 \text{ MeV} \leq E_0 \leq 1000 \text{ MeV}$. Buildup thickness in front of counter: $2X_0$.

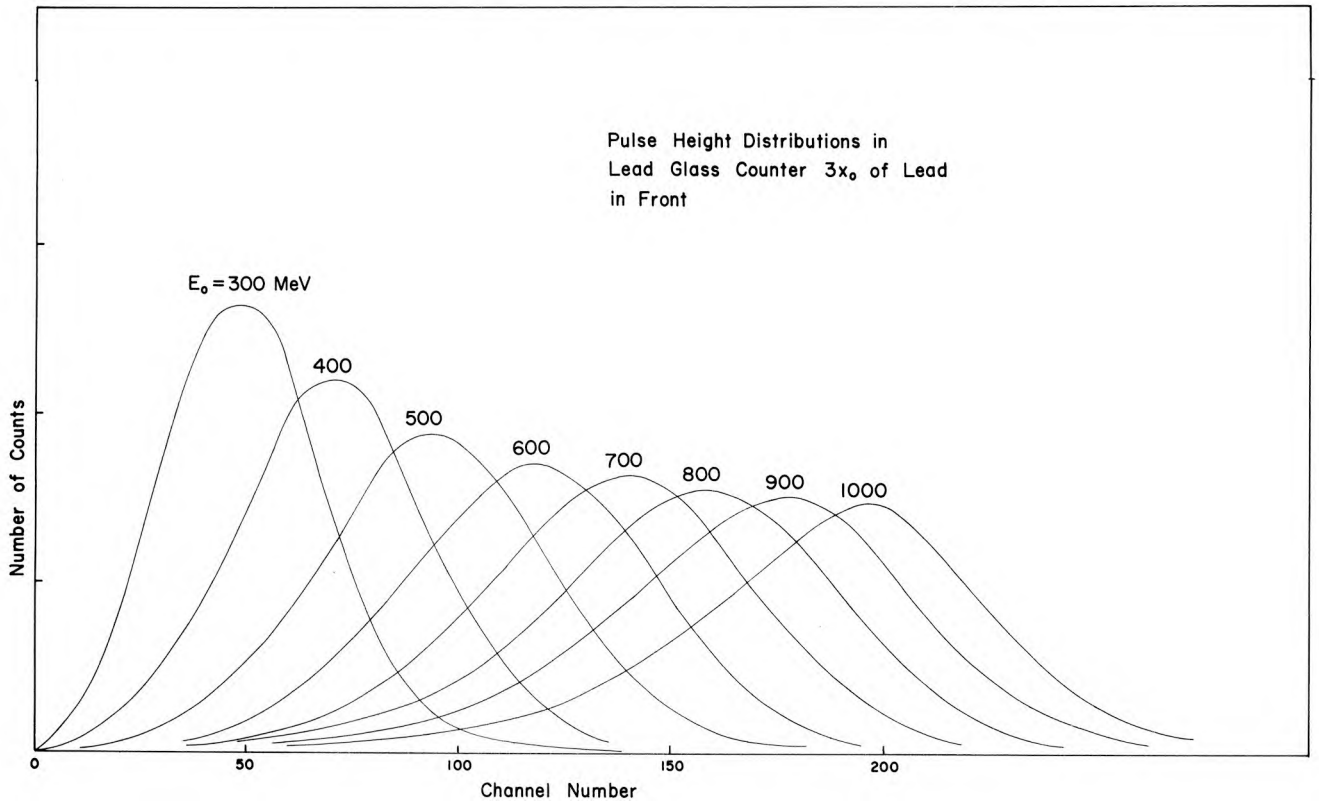


Figure 14 - Shower pulse height distributions from lead glass counter: $300 \text{ MeV} \leq E_0 \leq 1000 \text{ MeV}$. Buildup thickness in front of counter: $3X_0$.

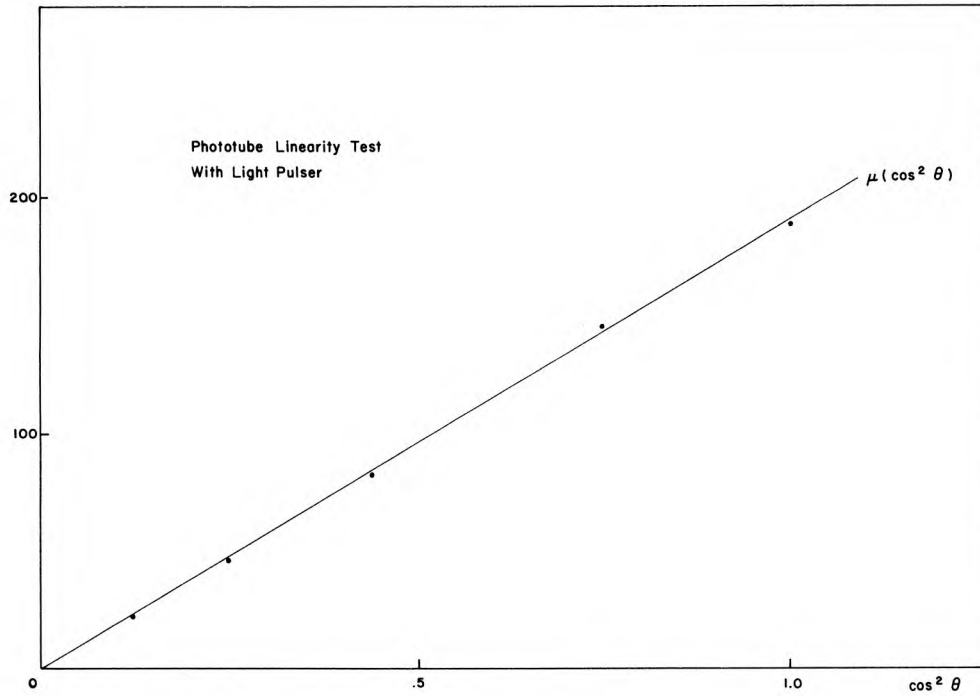


Figure 15 - Light pulser check on linearity of phototube response: pulse height maxima as a function of polaroid setting. Intensity of light input: $I \approx \text{const.} \times \cos^2 \theta$.

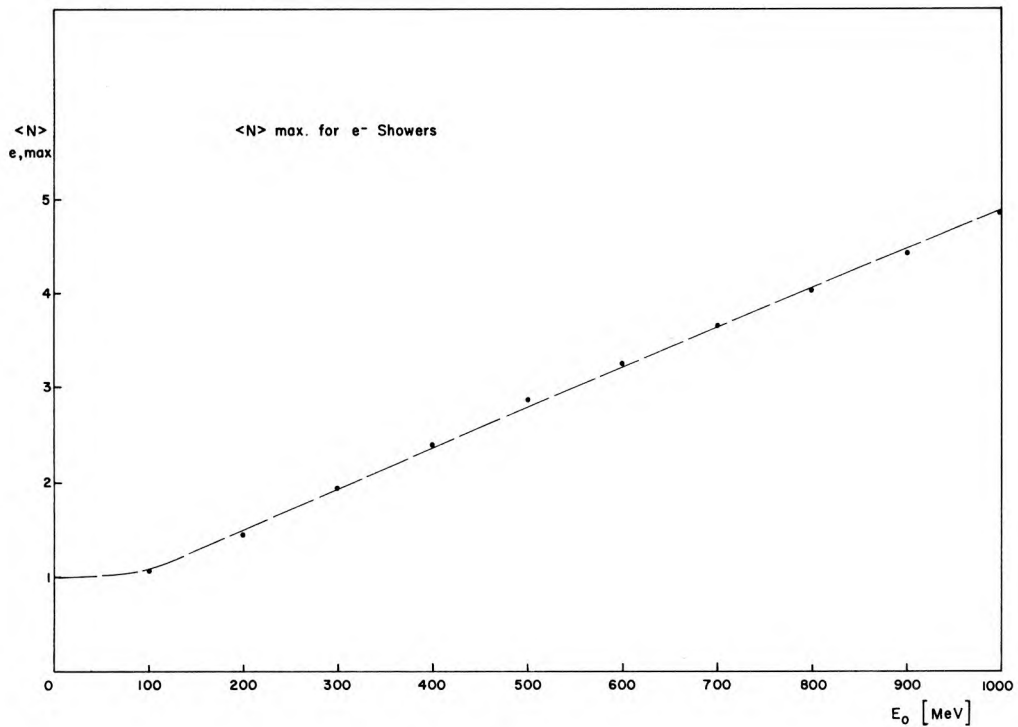


Figure 16 - Average number of shower particles, at location of shower maximum, as a function of incoming electron energy. For $E_0 \geq 100$ MeV, $\langle N \rangle$ rises close to linearly.

